

Supporting Information

Batchelor et al. 10.1073/pnas.1318022110

SI Materials and Methods

Study Design. Data were obtained from two prospective, concurrent clinical trials performed at the Massachusetts General Hospital Cancer Center and the Dana Farber Cancer Institute, Boston, MA. In one study, 46 newly diagnosed glioblastoma (nGBM) patients received 6 wk of fractionated radiation with daily temozolomide. One month following the completion of chemoradiation, temozolomide resumed at 150–200 mg/m² for 6 mo. Starting with day 1 of chemoradiation, cediranib (30 mg) was taken without interruption until disease progression or toxicity (Fig. 1 and Table S1). Standard eligibility criteria were used and all patients were required to have at least 1 cm in diameter of contrast-enhancing tumor to participate. The first six patients were enrolled in a run-in phase Ib study to determine the safety of the combination therapy and did not undergo the weekly and then monthly MRI and blood biomarker studies outlined below, so were not included in the imaging and circulating biomarker analyses. Thus, 40 patients enrolled in the phase II portion of the study and were included in the perfusion, vessel architectural imaging (VAI) and circulating biomarker analysis. Fourteen separate patients with nGBM were enrolled in a parallel imaging trial with the same main eligibility criteria and received the same chemoradiation, but did not receive cediranib or any other investigation agent with chemoradiation. These patients underwent imaging at similar time points as those participating in the cediranib study. Both studies (NCT00662506 and NCT00756106) were approved by the Institutional Review Board of Dana-Farber/Harvard Cancer Center and informed consent was obtained from all patients.

MRI Acquisition. All patients underwent scanning on a 3 Tesla MRI system (TimTrio, Siemens Medical Solutions). All patients were scanned twice before the start of chemoradiation (3–7 d and then 1 d before the start of chemoradiation and cediranib), day 1 after start of treatment, and then weekly until day 50. Following chemoradiation, patients were scanned monthly for 14 mo or until disease progression or toxicity. After 14 mo, MRIs were performed every other month. MRI scans included scout, pre- and postcontrast T1-weighted images, fluid-attenuated inversion recovery (FLAIR), dynamic susceptibility contrast (DSC) imaging, dynamic contrast-enhanced (DCE) imaging, and diffusion tensor imaging (DTI).

MRI Sequence Acquisition. Scout. The “AutoAlign” method of producing scout images was used to improve scan-to-scan reproducibility. Briefly, this method acquires two low-resolution whole-head scans (2.5-mm isotropic voxels) at different flip angles within 46 s, and uses a computer algorithm to compare the current location of the head with a predefined atlas. This localization is then used to ensure that the slice prescriptions are identical between scan sessions, even across many months (1, 2). **FLAIR images.** Axial FLAIR images were acquired with a TR = 10,000 ms, TE = 70 ms, 5-mm slice thickness, 1-mm interslice gap, 0.43-mm in-plane resolution, 23 slices, and a 512 × 512 matrix.

T1 images. Axial images were obtained before the injection of contrast. TR = 600 ms, TE = 12 ms, 5-mm slice thickness, 1-mm interslice gap, 0.43-mm in-plane resolution, 23 slices, and a 512 × 512 matrix.

DCE. To estimate precontrast T1 relaxation rates in the tissue, fast-gradient echo images were acquired before the injection of contrast agent with a TR = 7.3 ms, TE = 4.4 mm, 2.11-mm slice thickness, 0-mm interslice gap, 20 slices, 1.8-mm in-plane reso-

lution, and a 128 × 128 matrix, field-of-view 230 × 230 mm². This sequence was repeated five times at five different flip angles of 2°, 5°, 10°, 20°, and 30°. Fast-gradient echo images were then acquired with a TR = 6.8 ms, TE = 2.73, 2.11-mm slice thickness, 0-mm interslice gap, 20 slices, 1.8-mm in-plane resolution, 128 × 128 matrix, field-of-view 230 × 230 mm², and a flip angle of 10°. A total of 50–60 frames with these parameters were collected for up to 6 min. A bolus of 0.1 mMol/kg of GD-DTPA (gadopentetic acid) was injected after 52 s.

DSC. A combined gradient-echo and spin-echo EPI sequence was performed to enable relative vessel size mapping (3, 4). This sequence was acquired at a TR = 1,480 ms, TE1/TE2 = 32/93 ms, 5-mm slice thickness, 1.5-mm interslice gap, 12 slices, 1.2-mm in-plane resolution, and a 160 × 160 matrix, field-of-view 768 × 768 mm². A total of 120 frames with these parameters were collected up to 2.5 min. A bolus of 0.1 mMol/kg of GD-DTPA was injected after 80 s.

Postcontrast T1-weighted imaging. Axial T1-weighted images were acquired exactly as precontrast, as described above.

MRI Analysis. Volumetrics. Enhancing lesions and areas of T2 abnormality on FLAIR images were quantitatively analyzed by an experienced neuroradiologist blinded to patient identity, the order of the scans, and treatment status of the patients. The lesions were outlined using a volumetric approach described previously (5) that includes outlining each enhancing voxel on postcontrast scans and then summing the voxels to calculate an overall lesion volume.

Map synthesis. Blood perfusion maps were generated in nordicICE using DSC data. In addition to postprocessing leakage correction, the contrast agent pre-dose from DCE was used to saturate leaky tissue from blood-brain barrier breakdown or resection, thereby minimizing T1-shortening effects (6). Patient-specific variations were reduced by automatic arterial input function selection and partial volume correction and tumor DSC values were normalized to normal-appearing gray and white matter tissue (7). The DCE data were processed to create K^{trans} maps, a measure of the permeability-surface area product (8). Apparent diffusion coefficient maps were calculated from the DTI data (8).

VAI analysis. VAI was performed using microvessel and macrovessel DSC data as previously described (9). VAI analysis reflects vessel caliber and tissue oxygenation by exploiting the temporal shift in magnetic resonance signal that forms the basis for vessel caliber estimation. When visualized in a scatter plot, the resulting point-by-point temporal microvessel and macrovessel tissue-concentration curves will form a vortex where the blood volume corrected vortex area scales with the level of deoxygenated blood and is assumed proportional to the oxygen saturation (SO₂) level of the tissue, as previously shown (9). Changes in tumor Δ SO₂ levels were independent of the respective changes in vessel calibers.

06-Methyl Guanine Methyl Transferase Analysis. 06-methyl guanine methyl transferase (MGMT) promoter status was evaluated by methylation-specific PCR after bisulfate treatment using a standardized clinically validated protocol at the Department of Pathology, Massachusetts General Hospital.

Analyses of Receptor Tyrosine Kinase Gene Amplification in nGBM Tissue Specimens. We used probes for EGFR (CTD-2113A13 Spectrum Red or Green, Invitrogen Nick translation Kit), hepatocyte growth factor receptor (MET, CTB-1013N12 Spectrum rGreen, Invitrogen, Nick translation Kit), and platelet-derived

growth factor receptor- α (PDGFRA, RP11-58C6 Spectrum Red or Green, Invitrogen Nick Translation Kit). Two FISH reactions were performed with a mix of two probes (3 mL per slide), followed by denaturation of the probe and target at 80 °C for 5 min and overnight hybridization at 37 °C. Cell nuclei were counterstained with 4',6-diamidino-2-phenylindole and slides were evaluated using an Olympus BX61 fluorescent microscope. GBM genotype was determined after evaluation of 100 cell nuclei.

Circulating Biomarkers. Blood samples were collected in EDTA-containing tubes before and after cediranib-chemoradiation therapy at days 1, 2, and 14, and then weekly until the end of combination therapy (week 10). Plasma samples were separated by centrifugation, then aliquoted and stored at -80 °C until they were used for ELISA measurements. Measurements were carried out for circulating VEGF, plasma growth factor (PIGF), sVEGFR1, and basic FGF using the Human Angiogenesis Panel 1 Kit (K15190D) from Meso-Scale Discovery, as previously described (10). Soluble VEGFR2, stromal cell-derived factor 1 α (SDF1 α), carbonic anhydrase IX (CAIX), and Ang-2 were measured using ELISA kits from R&D Systems. Every sample was run in duplicate.

Statistical Analysis. A change in log-transformed perfusion measurement had to be higher or lower than the 95% confidence interval of the variations across patients (derived from the within-patient perfusion changes between the two baseline time points) as previously described for recurrent GBM patients treated with cediranib alone (6). An increase or decrease in perfusion had to persist for two or more time points. Groups were compared using exact Mann-Whitney and Fisher tests (for comparisons of circulating biomarkers and genotypes) as well as stratified log-rank test and Wald test in Cox regression analysis with log-transformed covariates (for survival data). Biomarker changes were expressed as ratios, reported as median with interquartile intervals, and tested using exact paired Wilcoxon test. We considered each biomarker separately, and used the method of Genovese et al. to control the false-discovery rate (FDR) at 5% in multiple statistical tests performed over time (11). *P* values of less than 0.05 were considered statistically significant. Patients with missing data were excluded from the analysis, except for missing *MGMT* status (*n* = 9), which was considered as a separate stratum in the stratified analysis of survival.

1. Benner T, et al. (2006) Comparison of manual and automatic section positioning of brain MR images. *Radiology* 239(1):246–254.
2. van der Kouwe AJ, et al. (2005) On-line automatic slice positioning for brain MR imaging. *Neuroimage* 27(1):222–230.
3. Dennie J, et al. (1998) NMR imaging of changes in vascular morphology due to tumor angiogenesis. *Magn Reson Med* 40(6):793–799.
4. Pathak AP, et al. (2001) MR-derived cerebral blood volume maps: Issues regarding histological validation and assessment of tumor angiogenesis. *Magn Reson Med* 46(4):735–747.
5. Sorensen AG, et al. (2001) Comparison of diameter and perimeter methods for tumor volume calculation. *J Clin Oncol* 19(2):551–557.
6. Sorensen AG, et al. (2012) Increased survival of glioblastoma patients who respond to antiangiogenic therapy with elevated blood perfusion. *Cancer Res* 72(2):402–407.
7. Bjørnerud A, Emblem KE (2010) A fully automated method for quantitative cerebral hemodynamic analysis using DSC-MRI. *J Cereb Blood Flow Metab* 30(5):1066–1078.
8. Sorensen AG, et al. (2009) A “vascular normalization index” as potential mechanistic biomarker to predict survival after a single dose of cediranib in recurrent glioblastoma patients. *Cancer Res* 69(13):5296–5300.
9. Emblem KE, et al. (2013) Vessel architectural imaging identifies cancer patient responders to anti-angiogenic therapy. *Nat Med* 19(9):1178–1183.
10. Batchelor TT, et al. (2010) Phase II study of cediranib, an oral pan-vascular endothelial growth factor receptor tyrosine kinase inhibitor, in patients with recurrent glioblastoma. *J Clin Oncol* 28(17):2817–2823.
11. Genovese CR, Roeder K, Wasserman L (2006) False discovery control with *P*-value weighting. *Biometrika* 93:509–524.

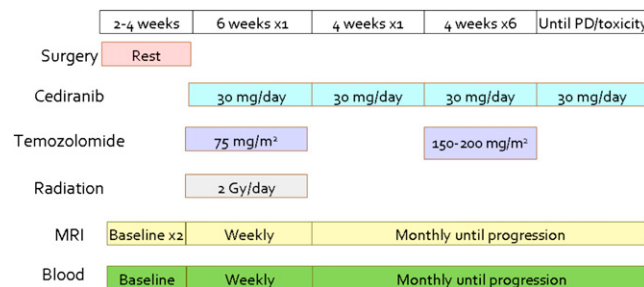


Fig. S1. Clinical study design.

Table S3. Plasma cytokines (pg/mL) that significantly change after cediranib with chemoradiation in newly diagnosed glioblastoma patients

Biomarker	Pre-Tx	Day 1	Day 2	Day 15	Day 22	Day 29	Day 36	Day 43
Plasma VEGF	139 [100,184] (N=39)	129 [101,192] (N=39)	138 [99,204] (N=39)	159 [128,234] (N=39)	168 [122,238] (N=38)	180 [141,229] (N=40)	173 [131,257] (N=36)	171 [129,263] (N=38)
P-value	N/A	0.17	0.99	0.11	0.077	0.0028	0.017	0.0056
Plasma PIGF	19 [15,23] (N=39)	25 [20,36] (N=39)	29 [22,39] (N=39)	41 [25,62] (N=39)	48 [34,65] (N=38)	50 [30,79] (N=40)	48 [35,65] (N=36)	45 [33,95] (N=38)
P-value	N/A	<0.0001	<0.0001	<0.0001	<0.0001	<0.0001	<0.0001	<0.0001
Plasma bFGF	57 [42,100] (N=39)	42 [28,84] (N=39)	45 [32,74] (N=39)	56 [40,87] (N=39)	52 [33,82] (N=38)	46 [26,71] (N=40)	56 [27,68] (N=36)	41 [27,82] (N=38)
P-value	N/A	0.067	0.0083	0.85	0.022	0.013	0.073	0.018
Plasma sVEGFR1	120 [102,143] (N=39)	92 [74,123] (N=39)	110 [93,141] (N=39)	103 [83,131] (N=39)	105 [85,140] (N=38)	101 [83,135] (N=40)	103 [89,127] (N=36)	105 [93,127] (N=38)
P-value	N/A	<0.0001	0.0052	<0.0001	0.0145	0.0018	0.0007	0.0024
Plasma sVEGFR2	5377 [4565,5758] (N=39)	4936 [4255,6105] (N=39)	4822 [4243,5745] (N=39)	4988 [4219,5866] (N=39)	4268 [3584,5005] (N=38)	4162 [3341,4683] (N=40)	4051 [3074,4552] (N=36)	4081 [3221,4926] (N=38)
P-value	N/A	0.16	0.0002	0.0015	<0.0001	<0.0001	<0.0001	<0.0001
Plasma Ang2	403 [296,496] (N=39)	372 [296,553] (N=39)	372 [296,585] (N=39)	372 [260,493] (N=39)	292 [206,433] (N=38)	388 [205,534] (N=40)	348 [251,455] (N=36)	327 [183,538] (N=38)
P-value	N/A	0.32	0.039	0.0001	0.0002	0.064	0.070	0.035
Plasma SDF1α	1433 [1158,2086] (N=39)	1461 [1010, 1968] (N=39)	1510 [1226,2070] (N=39)	1517 [1248,2111] (N=39)	1759 [1234,2120] (N=38)	1569 [1279,2107] (N=40)	1826 [1347, 2223] (N=36)	1861 [1417,2204] (N=38)
P-value	N/A	0.15	0.14	0.099	0.049	0.053	0.024	0.0025
Plasma IL-6	1.44 [0.85,2.14] (N=39)	1.40 [0.99,1.73] (N=39)	1.57 [1.14,2.07] (N=39)	1.60 [0.96,2.55] (N=39)	1.40 [0.91,1.98] (N=38)	2.06 [1.10,3.33] (N=40)	2.22 [1.20,3.23] (N=36)	2.07 [1.41,3.26] (N=38)
P-value	N/A	0.98	0.17	0.64	0.72	0.013	0.012	0.032
Plasma IL-8	4.61 [3.70,5.98] (N=39)	4.62 [3.67,5.71] (N=39)	5.02 [3.79,6.01] (N=39)	4.83 [3.65,6.18] (N=39)	4.93 [3.66,6.21] (N=38)	5.16 [3.82,7.45] (N=40)	5.33 [4.02,6.78] (N=39)	5.37 [4.91,6.41] (N=38)
P-value	N/A	0.22	0.33	0.52	0.77	0.14	0.98	0.023
Plasma TNF-α	8.1 [6.6,10.7] (N=39)	7.7 [6.2,11.2] (N=39)	8.4 [6.5,10.8] (N=39)	9.2 [7.3,10.8] (N=39)	9.7 [7.8,11.7] (N=38)	11.0 [8.8,16.2] (N=40)	12.2 [9.3,13.5] (N=36)	12.5 [10.1,17.2] (N=38)
P-value	N/A	0.54	0.12	0.11	0.021	<0.0001	<0.0001	<0.0001
Plasma CAIX	31.9 [19.7,53.9] (N=39)	43.7 [20.5,60.9] (N=39)	40.6 [23.8,60.3] (N=39)	45.0 [25.5,80.5] (N=39)	58.2 [36.5,94.4] (N=38)	57.6 [32.1,94.5] (N=40)	68.8 [32.3,100.4] (N=36)	58.3 [36.5,80.6] (N=38)
P-value	N/A	0.20	0.17	0.0058	0.0004	<0.0001	0.0005	<0.0001

Data are shown as medians and interquartile ranges (in square brackets) and are compared with baseline (pretreatment, Pre-Tx) levels. Changes: increase highlighted in red, decrease in yellow.

¹P values are from the paired exact paired Wilcoxon test.

Table S4. Changes in PIGF in nGBM patients receiving chemoradiation treatment alone vs. chemoradiation treatment with cediranib

Time-point	Chemoradiation alone			Chemoradiation with cediranib			<i>P</i>	<i>P</i> _{adj} *
	Median	IQR	<i>n</i>	Median	IQR	<i>n</i>		
Baseline (pg/mL)	21	(20, 28)	13	19	(15, 23)	39	0.16	0.16
Week 1 (fold-change from baseline)	0.94	(0.85, 1.15)	14	1.84	(1.49, 2.53)	38	<0.0001	<0.0001
Week 2 (fold-change from baseline)	1.12	(1.06, 1.19)	12	2.38	(1.93, 2.90)	38	<0.0001	<0.0001
Week 3 (fold-change from baseline)	1.05	(0.97, 1.19)	14	2.37	(1.84, 3.55)	39	<0.0001	<0.0001
Week 4 (fold-change from baseline)	1.23	(1.09, 1.34)	12	2.46	(1.80, 3.46)	34	<0.0001	<0.0001
Week 5 (fold-change from baseline)	1.26	(1.12, 1.44)	14	2.83	(1.90, 5.42)	36	0.0001	0.0001
Week 6 (fold-change from baseline)	1.23	(1.19, 1.57)	13	3.05	(2.25, 3.58)	30	<0.0001	<0.0001

Data are shown as measured concentrations (for baseline) and fold-change from baseline values for weeks 1–6. IQR, inter-quartile range.

**P* values for comparison between studies are from the exact Mann–Whitney/Wilcoxon test; in the last column *P* values adjusted to control the FDR at 5%.

Table S5. Changes in plasma sVEGFR2 in nGBM patients receiving chemoradiation treatment alone versus chemoradiation treatment with cediranib

Time-point	Chemoradiation alone			Chemoradiation with cediranib			<i>P</i>	<i>P</i> _{adj} *
	Median	IQR	<i>n</i>	Median	IQR	<i>n</i>		
Baseline (pg/mL)	8,364	(7,892, 9,411)	13	5,377	(4,565, 5,758)	39	<0.0001	<0.0001
Week 1 (foldchange from baseline)	1.05	(1.00, 1.10)	14	0.95	(0.85, 1.02)	38	0.0014	0.0014
Week 2 (fold-change from baseline)	1.11	(1.00, 1.17)	12	0.82	(0.75, 0.89)	38	<0.0001	<0.0001
Week 3 (fold-change from baseline)	1.04	(0.96, 1.16)	14	0.76	(0.68, 0.89)	39	<0.0001	<0.0001
Week 4 (fold-change from baseline)	1.07	(0.95, 1.12)	12	0.76	(0.62, 0.85)	33	<0.0001	<0.0001
Week 5 (fold-change from baseline)	0.97	(0.94, 1.04)	14	0.75	(0.68, 0.88)	36	0.0001	0.0001
Week 6 (fold-change from baseline)	1.01	(1.00, 1.21)	12	0.70	(0.64, 0.82)	30	<0.0001	<0.0001

Data are shown as measured concentrations (for baseline) and fold-change from baseline values for weeks 1–6.

**P* values for comparison between studies are from the exact Mann–Whitney/Wilcoxon test; in the last column *P* values adjusted to control the FDR at 5%.

Table S6. Correlation between plasma PIGF and sVEGFR2 kinetics and changes in perfusion in nGBM patients treated with cediranib and chemoradiation

Time-point/biomarker	Plasma PIGF change		Plasma sVEGFR2 change	
	Stable or decreased perfusion	Increased perfusion	Stable or decreased perfusion	Increased perfusion
Baseline	N/A [18.9 pg/mL (15.5, 22.0) <i>n</i> = 20]	N/A [19.7 pg/mL (15.4, 30.4) <i>n</i> = 19]	N/A [5,562 pg/mL (4,833, 5,835) <i>n</i> = 20]	N/A [5,064 pg/mL (4,437, 5,554) <i>n</i> = 19]
AUC		0.56		0.61
<i>P</i> value		<i>P</i> = 0.55		<i>P</i> = 0.25
Day 1	1.26 (1.11, 1.54) (<i>n</i> = 19)	1.34 (1.18, 1.60) (<i>n</i> = 19)	0.964 (0.903, 1.059) (<i>n</i> = 19)	0.973 (0.892, 1.082) (<i>n</i> = 19)
AUC		0.61		0.51
<i>P</i> value		<i>P</i> = 0.27		<i>P</i> = 0.93
Day 2	1.28 (1.22, 1.65) (<i>n</i> = 19)	1.57 (1.32, 2.21) (<i>n</i> = 19)	0.957 (0.916, 1.015) (<i>n</i> = 19)	0.929 (0.909, 0.983) (<i>n</i> = 19)
AUC		0.64		0.60
<i>P</i> value		<i>P</i> = 0.15		<i>P</i> = 0.30
Day 8	1.63 (1.48, 1.97) (<i>n</i> = 20)	2.19 (1.79, 3.53) (<i>n</i> = 18)	0.996 (0.919, 1.025) (<i>n</i> = 20)	0.869 (0.831, 0.959) (<i>n</i> = 18)
AUC		0.71		0.73
<i>P</i> value		<i>P</i> = 0.024		<i>P</i> = 0.014
Day 15	2.03 (1.63, 2.49) (<i>n</i> = 19)	2.61 (2.11, 3.80) (<i>n</i> = 18)	0.874 (0.792, 0.908) (<i>n</i> = 19)	0.771 (0.694, 0.816) (<i>n</i> = 18)
AUC		0.74		0.74
<i>P</i> value		<i>P</i> = 0.011		<i>P</i> = 0.012
Day 22	1.99 (1.46, 2.64) (<i>n</i> = 20)	2.68 (2.36, 5.41) (<i>n</i> = 19)	0.863 (0.753, 0.974) (<i>n</i> = 20)	0.712 (0.606, 0.765) (<i>n</i> = 19)
AUC		0.78		0.82
<i>P</i> value		<i>P</i> = 0.0026		<i>P</i> = 0.0004
Day 29	1.84 (1.58, 2.36) (<i>n</i> = 18)	3.72 (2.59, 5.39) (<i>n</i> = 17)	0.780 (0.747, 0.910) (<i>n</i> = 17)	0.674 (0.532, 0.846) (<i>n</i> = 17)
AUC		0.85		0.69
<i>P</i> value		<i>P</i> = 0.0002		<i>P</i> = 0.058

Data are shown as fold-change from baseline values (with interquartile range) and area under the curve (AUC) values. For pretreatment measurements, data are shown as actual concentrations (in pg/mL). *P* values are from the exact Mann–Whitney/Wilcoxon test.

Table S7. Histological analysis of EGFR, PDGFR, MET amplification and correlation with progression-free and overall survival

RTK	Mosaic receptor tyrosine kinase (RTK) amplification (%)						
	EGFR	PDGFRA	MET	EGFR+ PDGFRA	EGFR+ MET	PDGFRA +MET	EGFR+ PDGFRA+ MET
Samples tested	45	31	31	31	31	31	31
Amplification detected	21 (46.7)	3 (9.7)	3 (9.7)	1 (3.2)	0	1 (3.2)	1 (3.2)
Overall survival	1.75 (0.86,3.75) <i>P</i> = 0.12	1.25 (0.36,4.28) <i>P</i> = 0.073	0.51 (0.07,3.87) <i>P</i> = 0.51	N/A	N/A	N/A	N/A
Progression-free survival	1.29 (0.66,2.50) <i>P</i> = 0.45	1.12 (0.33,3.85) <i>P</i> = 0.86	0.68 (0.09,5.09) <i>P</i> = 0.70	N/A	N/A	N/A	N/A

Data are shown as hazard ratios and 95% confidence intervals.

Table S8. Correlation between RTK amplification and changes in perfusion in nGBM patients treated with cediranib and chemoradiation

Tissue biomarker	Tumor genotype (%)	
	Stable or decreased perfusion	Increased perfusion
EGFR amplification	13/19 (68.4%)	6/20 (30%)
Odds ratio		0.2 (0.0, 0.9)
<i>P</i> value		<i>P</i> = 0.026
PDGFRA amplification	3/14 (21.4%)	0/13 (0%)
Odds ratio		0.0 (0.0, 2.5)
<i>P</i> value		<i>P</i> = 0.22
MET amplification	2/14 (14.3%)	0/13 (0%)
Odds ratio		0.0 (0.0, 5.7)
<i>P</i> value		<i>P</i> = 0.48

Data are shown as odds ratios with interquartile range. *P* values are from Fisher exact test.